

## RESPONSE AMPLITUDE OPERATORS OF TLP FLOATING WIND TURBINE - CALCULATIONS AND EXPERIMENTS

Ewelina CIBA<sup>\*</sup>, Filip HAHS\*, Miroslaw GRYGOROWICZ\*, Paweł DYMARSKI<sup>\*</sup>

\*Faculty of Mechanical Engineering, Gdańsk University of Technology, 11/12 Gabriela Narutowicza Street, 80-233 Gdańsk

[ewelina.ciba@pg.edu.pl](mailto:ewelina.ciba@pg.edu.pl), [filip.hahs@pg.edu.pl](mailto:filipl.hahs@pg.edu.pl), [miroslaw.grygorowicz@pg.edu.pl](mailto:miroslaw.grygorowicz@pg.edu.pl), [pawel.dymarski@pg.edu.pl](mailto:pawel.dymarski@pg.edu.pl)

received 01 April 2025, revised 03 November 2025, accepted 03 November 2025

**Abstract:** The paper presents the results of experimental studies of the motion of a TLP type wind platform on a regular wave and the results of calculations in the Ansys AQWA program. Two different available methods of modeling additional damping related to viscosity were used, i.e. linear damping and quadratic (Morison) damping. The damping coefficients were determined based on RANSE CFD calculations of forced oscillations of the platform for different frequencies and amplitudes. The obtained values indicate that the use of the quadratic coefficient gives more accurate results. This is due to the fact that its value does not change significantly depending on the frequency and amplitude of the excitation, in contrast to the linear coefficient, where the observed differences are significant.

**Key words:** Floating Offshore Wind Platform (FOWP), Response Amplitude Operators (RAO), hydrodynamic coefficient, Tension Leg Platform (TLP)

### 1. INTRODUCTION

Offshore wind energy is developing very quickly. New platform concepts are constantly emerging, such as the floating platform with a horizontal axis turbine described by Grzelak [1]. Familiar and well-documented platforms are also being developed and modified: the classic semi-submersible platform, commonly used in the oil industry; the spar platform, which operates using the same principle as a fishing float; and the Tension Leg Platform (TLP), in which the force restoring the equilibrium position results from the positive difference in buoyancy and the mass of the structure.

The increase in power production demands cause the required turbine size to grow, which necessitates the use of greater operational depths. Beyond a certain limit, fixed-foundation platforms stop being practical and designers must move to floating structures. Along with the development of new concepts for wind turbine platforms, new techniques for estimating their motion have been created. These methods can be divided into three main groups: model tests, RANSE-CFD calculations and calculations based on boundary methods. The third method requires the least time and power, but to obtain correct results it must take into account hydrodynamic coefficients related to viscosity. There are many examples of such an approach in the literature. Ciba et al. [2] show how a 3 column spar platform can be modeled using the boundary element method, extended with linear damping coefficients determined on the basis of experimental studies. Otori et al. [3] presented the results of numerical calculations of coefficients for a Barge platform. The correctness of their calculations was confirmed by the results of the conducted experiments. Bhinder et al. [4] presented a methodology for identifying and considering the drag damping force in potential flow models that is consistent with CFD simulations. Dadmarzi et al. [5] considered the problem of forces acting on a restrained structure to identify the contribution of viscous forces. For this purpose, they used CFD solutions to calculate the forces on the columns and

potential flow to extract Morison coefficients. Zhang and Paterson [6] compared the hydrodynamic forces determined by RANSE CFD calculations and the Morison equation using the strip theory, noting that in this case the forces determined by the strip theory are underestimated. They pointed out the reason for this to the fact that the Morison equation neglects diffraction effects. Clement et al. [7] investigated the influence of viscous damping on the motion of a floating hybrid platform, finding it significant for the pitch motion. The influence of viscous damping was presented by Ciba and Dymarski [8] who presented the calculation of hydrodynamic coefficients for heave plates. The results presented in the paper were obtained based on RANSE CFD calculations using a forced oscillation method. Another method of determining hydrodynamic coefficients, based on the forces acting on a stationary object placed in an oscillatory flow, was presented by Dymarski et al. [9].

Determination of hydrodynamic coefficients is a subject of analysis not only in the case of floating platforms. There are many works available in the literature concerning underwater vehicles, such as those presented by Hong et al. [10] or experimentally supported calculations by Cely et al. [11]. Landmann et al. [12] determined coefficients allowing modeling of ropes covered with crustaceans.

The research and calculations presented in this article concern the Tension Leg Platform (TLP). These platforms are characterized by an excess of buoyancy in relation to mass, which causes constant tension in the anchor ropes. This tension is responsible for the creation of a restoring force, which causes the platform to return to its equilibrium position after the load acting on it is removed. A major advantage of this type of platform is the vertical method of anchoring, which significantly narrows the area of the platform installation when compared to traditional anchor chains, which are usually placed far from the platform axis. Another good feature of the discussed type of platform is its ease of parametric design, allowing the selection of the length of the tendons and the excess buoyancy to adapt the structure to the operating conditions. By changing the

length of the tendons and their tension, we can influence the frequency of free oscillations of the platform, and thus minimize the phenomenon of resonance on the wave.

The values of the hydrodynamic coefficients for the TLP platform consisting of 4 horizontal and 4 vertical cylinders were presented by O'Kane et al. [13]. Ren et al. [14] presented analyses of the TLP platform performed in the AQWA and WAMIT programs. They do not mention additional viscosity coefficients, which may be the reason for the significant motion of the platform. Zhou et al. [15] presented analyses of the TLP platform performed in the Ansys AQWA program. However, based on the presented free oscillation tests, it can be seen that no additional damping was taken into account, because the oscillation decay is small or nonexistent, contrary to what the experiments show for this type of structure. Very good analyses and high convergence of calculations with the experiment were presented by Vardaroglu et al. [16] who determined the hydrodynamic coefficients based on free oscillation tests. Pegasalajar-Jurado et al. obtained similarly good results. [17] calibrating the computational model based on the results obtained by free oscillations for a 10 MW TLP turbine. However, they noticed that introducing frequency-dependent coefficients could improve the accuracy of the obtained computational results. The results of interesting model studies of the TLP platform for waves at different angles of inflow were presented by Jin et al. [18]. The analysis of the literature shows that in order to obtain correct results of simulations of floating objects using simplified models, coefficients related to viscosity should be included in them.

## 2. ANALYZED PLATFORM

The tested platform was designed for a 15 MW wind turbine, in the Baltic Sea area with a depth of 70 m. Its shape is shown in Fig. 1, and the basic data are presented in Table 1.

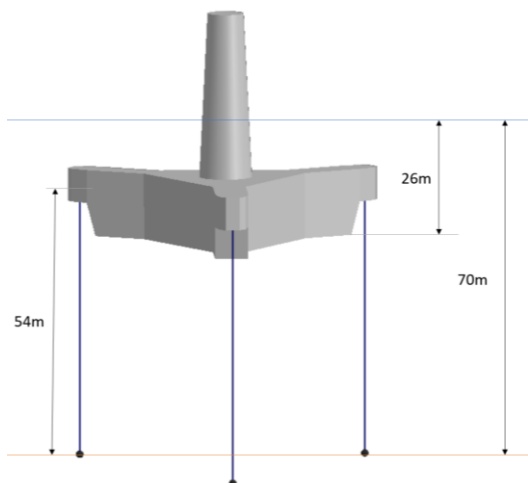


Fig. 1. The shape of the analyzed TLP platform

Tab. 1. Platform parameters

Mass [t]	3555.3
Displacement [m <sup>3</sup> ]	12 150
Draft [m]	26
Length of leg [m]	54
Water depth [m]	70

The research was carried out on a 1:65 scale platform model in a 40x4x3 m model pool at the Gdańsk University of Technology, equipped with a plate and an 8-segment regular and irregular wave generator, capable of recreating a given wave spectrum, with a maximum wave height of 0.25 m, designed and made by Edinburgh Design. Platform displacements were measured by a Qualisys system based on high-speed cameras, capable of determining the position and orientation of an object in 6 degrees of freedom. 6D object, to an accuracy of 0.4 mm.

The experimental setup is shown in Fig. 2.

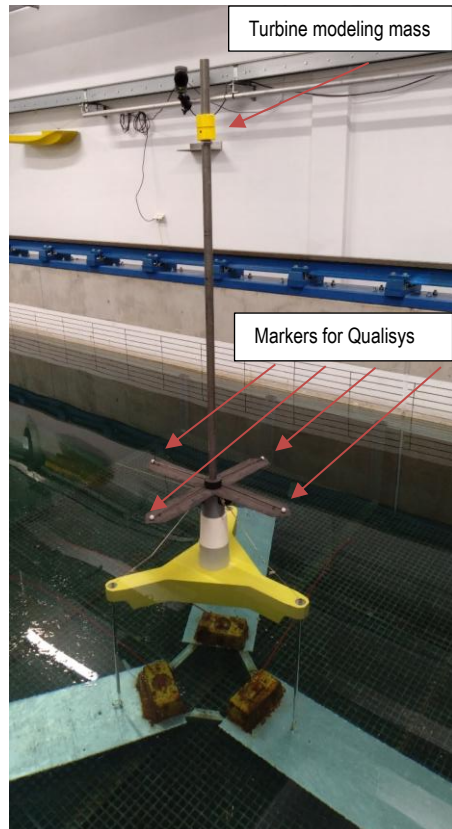


Fig. 2 Model of the tested platform

A commonly used method for assessing the behavior of a platform in marine conditions is to determine its amplitude characteristics, i.e. the response of the structure in relation to the frequency of the forcing wave. In this process, the behavior of the object on a regular wave is examined and based on the obtained results, it is possible to predict the movement for a given spectrum of an irregular wave. Depending on the type of platform, its movements in different degrees of freedom may be of interest. In the case of the TLP platform, the horizontal movement in the X direction is considered to be most important.

In the Ansys AQWA program the user has the ability to determine the platform motion for various environmental excitations. The calculations are based on the boundary element method without taking into account viscosity. To take viscous effects into account, an additional coefficient matrix must be introduced.

In the case of a TLP type platform, we will be mainly interested in the horizontal movement, for which we can write (1).

$$(m + A_{11})\ddot{x} + B_{eq11}\dot{x} + C_{11}x = F_1 \quad (1)$$

Where  $A_{11}$ -added mass on x direction,  $B_{eq11}$ - damping

coefficient on x direction,  $C_{11}$ - stiffness coefficient for TLP  $C_{11} = \frac{1}{L_t}(\rho g V - mg)$  Lt- length of leg

After separating the damping term into a linear and quadratic part, the equation will then have the form (2).

$$(M + A_{11})\ddot{x} + B_{11}\dot{x} + \frac{1}{2}\rho C_{D_{11}}A\dot{x}|\dot{x}| + C_{11}x = F_1 \quad (2)$$

The Ansys AQWA program calculates part of the Beq attenuation coefficient based on the diffraction theory, but the viscous part is omitted. Hence, the user has the option of introducing additional attenuation, in the form of a matrix of linear additional attenuation coefficients Badd, or quadratic Morison additional attenuation coefficients CD.

Calculations performed without the additional damping term give greatly overestimated values of platform movements in relation to the actual ones, so this is a step that cannot be omitted.

The methods for determining hydrodynamic coefficients are presented in the diagram below (fig. 3).

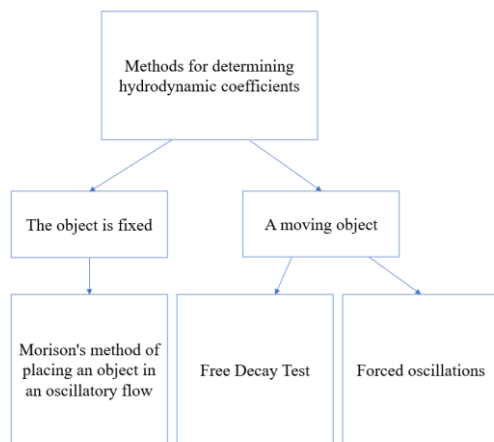


Fig. 3. Division of methods for determining hydrodynamic coefficients depending on the way of defining the variable speed

In the case of RANSE CFD calculations, the forced oscillation method is the best as it allows determining the value of the coefficients depending on the forcing period, while the free oscillation method only provides the value of the coefficients for the free oscillation period of the object. Moreover, the free oscillation method gives higher values of the damping coefficients, due to the decreasing amplitudes of successive oscillations. The use of oscillatory flow in the case of RANSE CFD calculations may cause numerical discrepancies.

For model tests, the free oscillation method is preferred, as it does not require the use of an additional motion forcing device, relying only on an initial forcing. The disadvantage of this method is the great difficulty in isolating the motion in a single degree of freedom. The appearance of additional coupled motions changes the values of the determined coefficients.

### 3. DETERMINATION OF HYDRODYNAMIC COEFFICIENTS BY FORCED OSCILLATION METHOD

The first stage of the calculations was to determine the hydrodynamic coefficients of the platform using forced oscillation tests. The calculations were performed using the STAR CCM+ program based on the RANSE CFD method.

The main features of the model are:

- Volume of Fluid model (Fig. 4) allowing for modeling of two-phase flow,

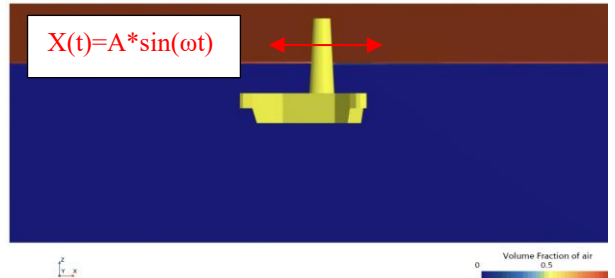


Fig. 4. View in the plane of symmetry, blue color - volume cell completely filled with water, red color - volume cell filled with air

- Overset mesh (Fig. 5) allowing the object to move along a given trajectory,

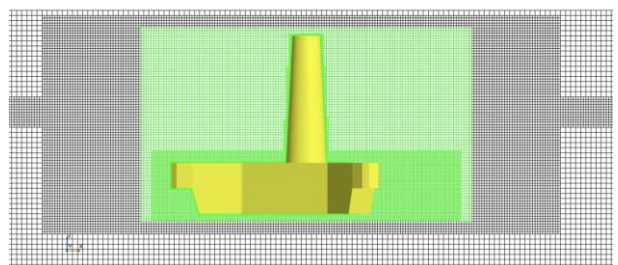


Fig. 5. View of the mesh in the plane of symmetry, divided into a moving mesh - marked in green and a stationary mesh - marked in black

- K-ε turbulence model.

The computational mesh was refined in the platform's motion region and on the free surface. To enable the representation of the large velocity gradient at the platform walls, a prismatic mesh composed of five layers was constructed. A free-slip wall condition was assumed for the walls surrounding the stationary domain, and an atmospheric pressure inlet condition was assumed for the top of the domain. An overset mesh condition was assumed for the wall connecting the stationary and moving domains, allowing the program to determine conditions based on a given area of the stationary domain.

To check the independence of the mesh (fig. 6), calculations were performed for meshes with the following numbers of elements: 1 million, 10 million and 70 million. Since no significant difference was observed between the values of the coefficients obtained from calculations for 10 and 70 million, it was decided to perform calculations on a mesh with 10 million elements.

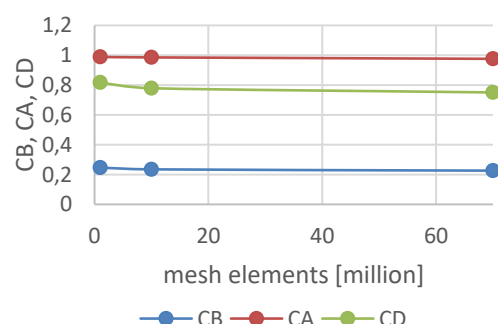


Fig. 6. The values of the determined coefficients depend on the number of mesh elements used for the calculations

The main difficulty in determining the hydrodynamic coefficients is that they can vary in time. The value of the hydrodynamic coefficients in oscillatory motion depends on both the amplitude of the motion and the frequency of the excitation. Because of this, a series of calculations had to be carried out, the results of which can be seen on Fig. 12. The hydrodynamic coefficients were determined by matching the force function acting on the moving object with the given amplitude and frequency using the least squares method. Comparing the individual runs, it was clearly visible that a force function based on the linear damping coefficient gives better results than one based on the quadratic (Morison) damping coefficient. However, the greatest differences do not appear at the moment when the velocity of the structure is the highest, but when the structure is affected by forces related to both velocity and acceleration. Example runs for an excitation amplitude  $A = 5 \text{ m}$  and frequency  $\omega = 0.4488 \text{ rad/s}$  are shown in Fig. 7. Additionally, the auxiliary axis shows the given velocity of the structure.

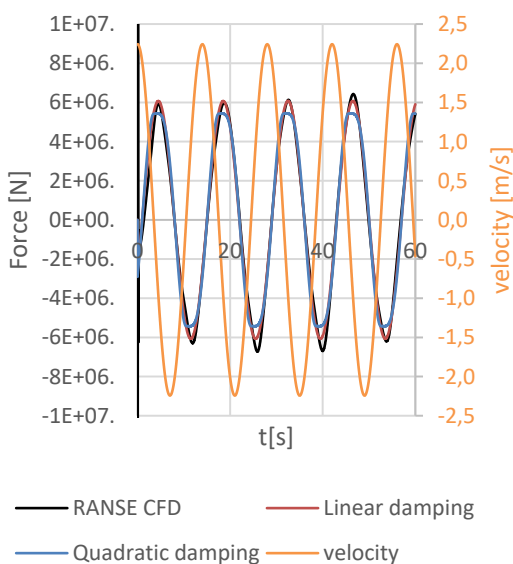


Fig. 7. The value of the force acting on an oscillating object obtained from calculations and its approximation using a linear and quadratic equation

The values of the dimensionless damping coefficient defined as  $C_B = B/(2V\rho\omega)$  are shown in the graph (Fig. 8).

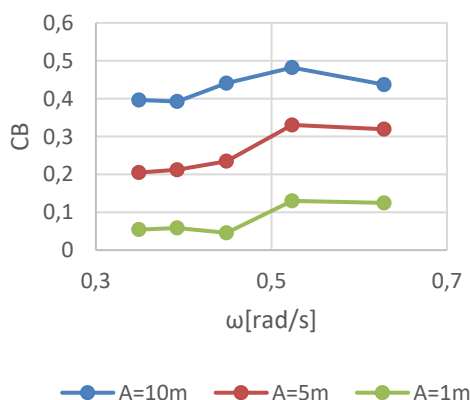


Fig. 8. Values of the dimensionless linear damping coefficient as a function of frequency for different motion amplitudes

The values of the added mass coefficient defined as  $C_A = A/(V\rho)$  are shown in Fig. 9.

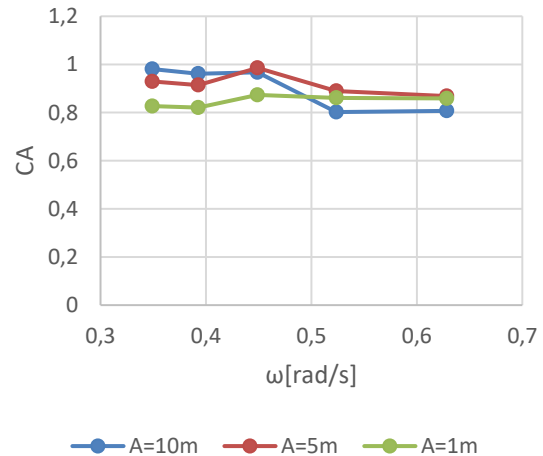


Fig. 9. Values of the dimensionless added mass coefficient depending on the frequency for different motion amplitudes

The values of the Morison drag coefficient are shown in the graph (Fig. 10).

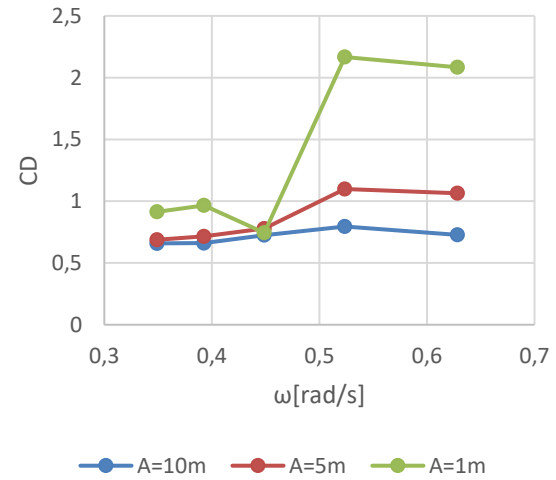


Fig. 10. Morison coefficient values depending on the frequency for different movement amplitudes

#### 4. FREE OSCILLATION TEST COMPARISON OF CALCULATION AND EXPERIMENT RESULTS

A surface model, separated into above-water and below-water sections, was introduced into the ANSYS AQWA program. The geometry was divided into 3,500 elements (Fig. 11). The bottom depth and anchor line attachment points were defined.

Based on the determined values, the additional damping coefficients related to viscosity were entered into the program. Then, free oscillation tests were performed for different initial deflection amplitudes and the results were compared with experimental data (Fig. 12).

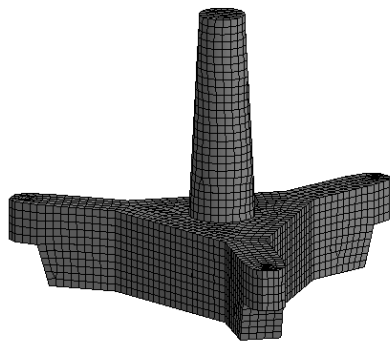
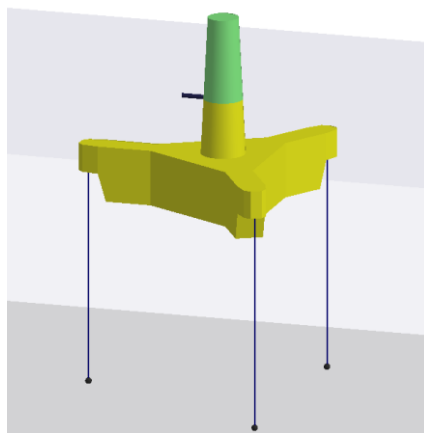
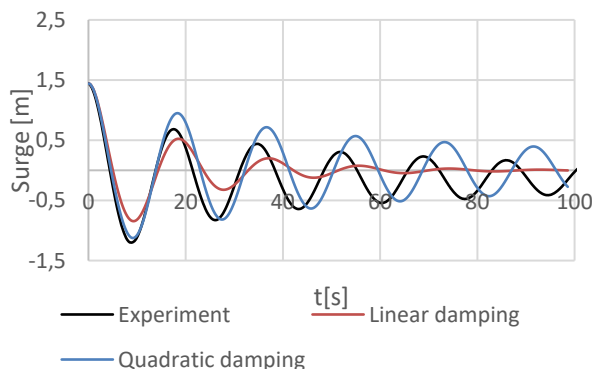
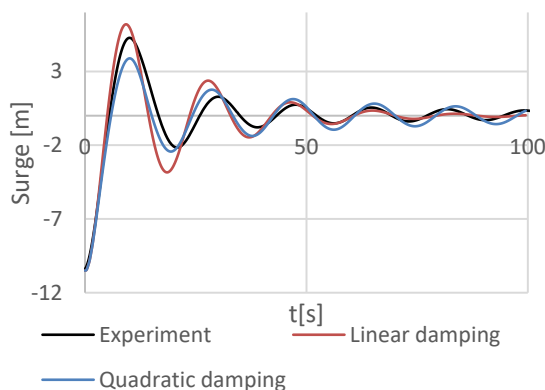


Fig. 11. Surface model divided into underwater and above-water parts, and its division into surface mesh elements

a)



b)



c)

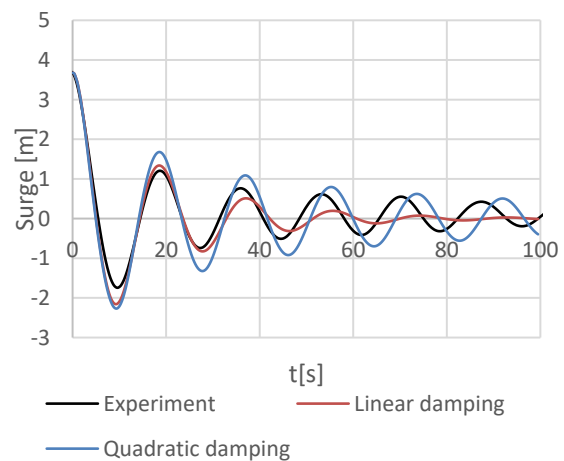


Fig. 12. Oscillation patterns of free structures for various initial deflections. Comparison of experimental results with calculations where damping is modeled using a linear or quadratic coefficient

Analyzing the results of free oscillations, it can be seen that the oscillations are very strongly dependent on the initial displacement of the structure. Therefore, none of the methods which assume a constant damping coefficient, achieve good accuracy when modelling late-time behaviour. It can also be seen that using linear coefficient causes the oscillations to die out much faster than when quadratic coefficients.

## 5. AMPLITUDE CHARACTERISTICS COMPARISON OF CALCULATION AND EXPERIMENT RESULTS

The platform's behavior was tested and calculated in the conditions of regular waves of different frequencies. The calculations were performed in the Ansys AQWA program using the linear and quadratic damping model. The results are presented in the graph in Fig. 13.

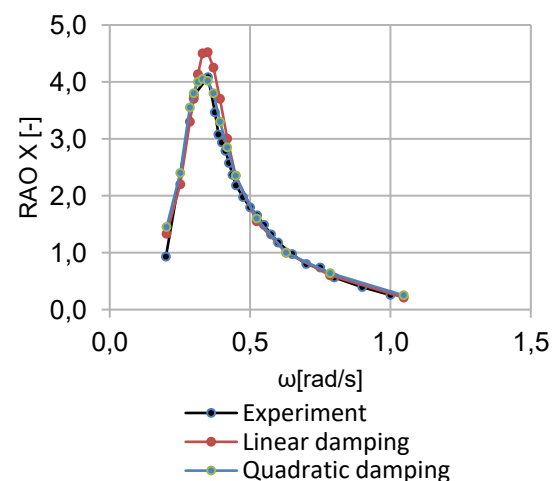


Fig. 13. Comparison of Response Amplitude Operators obtained from experimental studies of the platform motion on a regular wave and calculated using the program where the damping is modeled using a linear or quadratic coefficient

When comparing the results it can be seen that both linear and quadratic damping coefficients reproduce the experimental results well. However, the quadratic damping factor gives much better results in the region of the highest values of the Response Amplitude Operator. The largest difference between the measured value and the one calculated using the square factor was 1.5%, while the linear factor gave a difference of 11%.

## 6. CONCLUSIONS

Several important conclusions can be drawn from the calculations performed and their comparison with model tests:

- The method of determining hydrodynamic coefficients using forced oscillations, in which the coefficient values are determined based on the results of RANSE CFD calculations gives good results.
- Calculating the force acting on an object moving in oscillatory motion using a linear damping coefficient gives a more accurate result than using a quadratic coefficient.
- The value of the linear damping coefficient increases strongly with the increase in the amplitude of the excitation.
- Using a constant damping coefficient (both linear and quadratic) does not allow for very good prediction of the object's movements during the free oscillation test.
- It is possible to model the platform's motion with a reasonable degree of accuracy, using the boundary element method extended by the influence of viscosity by assigning an additional matrix of constant damping coefficients, although in reality their value depends on the amplitude and frequency of the oscillatory motion.
- Using a quadratic damping coefficient allows for more accurate calculations of the amplitude characteristics, because unlike the linear coefficient, it does not change significantly with the amplitude and frequency of the motion.

In summary, Ansys Aqwa, with its quadratic damping coefficients, is a very good tool for assessing platform behavior. The surface mesh is easy to create and doesn't require significant computational resources. This allows for long simulation times, which is particularly important when studying the behavior of objects under irregular wave conditions.

## REFERENCES

1. Grzelak J, Guijarro Carrillo L, Nakielski J, Piotrowicz M, Doerffer K. An Innovative Floating System with a Savonius Rotor as a Horizontal-Axis Wind Turbine. *Pol. Marit. Res.* 2024;31 2(122): 13-19. <https://doi.org/10.2478/pomr-2024-0017>
2. Ciba E, Dymarski P, Grygorowicz M. Analysis of the Hydrodynamic Properties of 3-Column Spar Platform for Offshore Wind Turbines. *Pol. Marit. Res.* 2022;29 2 (114):35-42. <https://doi.org/10.2478/pomr-2022-0015>
3. Otori H, Kikuchi Y, Rivera-Arreba I, Vire A. Numerical study of hydrodynamic forces and dynamic response for barge type floating platform by computational fluid dynamics and engineering model. *Oce. Eng.* 2023;284:115100. <https://doi.org/10.1016/j.oceaneng.2023.115100>
4. Bhinder M, Babarit A, Gentaz L, Ferrant P. Potential Time Domain Model with Viscous Correction and CFD Analysis of a Generic Surging Floating Wave Energy Converter. *Int. J. of Mar. Energy* 2015; 10:70-96. <https://doi.org/10.1016/j.ijome.2015.01.005ff>
5. Dadmarzi FH, Ommani B, Califano A, Fonseca N, Berthelsen PA. Investigating Morison Modeling of Viscous Forces by Steep Waves on

Columns of a Fixed Floating Offshore Wind Turbine (FOWT) Using Computational Fluid Dynamics (CFD). *J. Mar. Sci. Eng.* 2025; 13(264). <https://doi.org/10.3390/jmse13020264>

6. Zhang D, Paterson EG. A study of wave forces on an offshore platform by direct CFD and Morison equation. *E3S Web of Conferences* 5 2015. <https://doi.org/10.1051/e3sconf/2015050502>
7. Clement Ch, Kosleck S, Lie T. Investigation of viscous damping effect on the coupled dynamic response of a hybrid floating platform concept for offshore wind turbines. *Oce. Eng.* 2021; 225:108836. <https://doi.org/10.1016/j.oceaneng.2021.108836>
8. Ciba E, Dymarski P. Modelling of the Viscosity Effect of Heave Plates for Floating Wind Turbines by Hydrodynamic Coefficients. *Acta Mech. Autom.* 2023;17(3). <https://doi.org/10.2478/ama-2023-0054>
9. Dymarski P, Ciba E, Marcinkowski T. Effective method for determining environmental loads on supporting structures for offshore wind turbines. *Pol. Marit. Res.* 2016;23 1(89):52-60. <https://doi.org/10.1515/pomr-2016-0008>
10. Hong L, Wang X, Zhang D, Xu H. Numerical Study on Hydrodynamic Coefficient Estimation of Underwater Vehicle. *J. Mar. Cci. Eng.* 2022; 10(8):1049. <https://doi.org/10.3390/jmse10081049>
11. Cely JS, Saltaren R, Portilla G, Yakrangi O, Rodriguez-Barroso A. Experimental and Computational Methodology for Determination of Hydrodynamic Coefficients Based on Free Decay Test: Application to Conception and Control of Underwater Robots. *Sensors* 2019;19(17): 3631. <https://doi.org/10.3390/s19173631>
12. Landmann J, Flack Ch, Kowalsky U, Wuchner R, Hildebrandt A, Goseberg N. Hydrodynamic coefficients of mussel dropper lines derived from large-scale experiments and structural dynamics. *J. of Oce. Eng. and Mar. Energy* 2024;10:175-192. <https://doi.org/10.1007/s40722-023-00303-w>
13. O'Kane JJ, Troesch AW, Thiagarajan KP. Hull component interaction and scaling for TLP hydrodynamic coefficients. *Oce. Eng.* 2002; 29:513-532. [https://doi.org/10.1016/S0029-8018\(01\)00039-7](https://doi.org/10.1016/S0029-8018(01)00039-7)
14. Ren Y, Venugopal V, Shi W. Dynamic analysis of a multi-column TLP floating offshore wind turbine with tendon failure scenarios. *Oce. Eng.* 2022;245(110472). <https://doi.org/10.1016/j.oceaneng.2021.110472>
15. Zhou Y, Ren Y, Shi W, Li X. Investigation on a Large-Scale Braceless-TLP Floating Offshore Wind Turbine at Intermediate Water Depth. *J. Mar. Sci. Eng.* 2022;10(302). <https://doi.org/10.3390/jmse10020302>
16. Vardaroglu M, Gao Z, Avossa AM, Ricciardelli F. Validation of a TLP wind turbine numerical model against model-scale tests under regular and irregular waves. *Oce. Eng.* 2022;256:111491. <https://doi.org/10.1016/j.oceaneng.2022.111491>
17. Pegalajar-Jurado A, Hansen AM, Laugessen R, Mikkelsen RF, Borg M, Kim T, Heilskov NF, Bredmose H. Experimental and numerical study of a 10MW TLP wind turbine in waves and wind. *J. Phys.: Conf. Ser.* 753 092007. <https://doi.org/10.1088/1742-6596/753/9/092007>
18. Jin R, Jiang Y, Shen W, Zhang H, Geng B. Coupled dynamic response of a tension leg platform system under waves and flow at different heading angles: An experimental study. *Appl. Ocean Res.* 2021;115:102828. <https://doi.org/10.1016/j.apor.2021.102848>

The calculations were performed using the STAR CCM+ license granted by Siemens and ANSYS AQWA license granted by MESco Sp. z o.o., partially conducted using the TASK computational network.

Ewelina Ciba:  <https://orcid.org/0000-0002-9042-5234>

Paweł Dymarski:  <https://orcid.org/0000-0002-6033-0461>



This work is licensed under the Creative Commons BY-NC-ND 4.0 license.